E. Motor and propeller selection

E.1 Brushless motor basics

There are a number of different ideas and models for BLDC motors around on the internet and this approach is mainly based on the approach used in the MIT QPROP code (Drela, 2007) and the Micromo page on motor calculations (Micromo Micro Motion Solutions, 2010). The MIT approach requires knowledge of additional motor properties and does not clearly predict motor voltage and current, while the Micomo approach lacks precision.

In reality a BLDC motor is driven by a three phase pulsed current coming from an ESC. Properly calculating the speed, torque and consumption of this dynamic system is complicated; the time averaged properties, however, can be simplified to those of an equivalent brushed motor. In this equivalent brushed motor model the input voltage and current are assumed constant. This constant voltage and current is not the same as the voltage and current given to the ESC, nor the actual pulsed voltage and current fed from the ESC to the motor, and can be referred to as the motor DC equivalent voltage and current. For the rest of this document, all references to voltage and current refer only to the motor DC equivalent values and not the actual values, nor the values at the ESC.

To predict the consumption of the motor, both its rotational speed (ω) and its operating torque must be known. The speed is predominantly a function of the motor's voltage, while the torque depends on the load. In terms of RC planes, the user typically 'knows' or commands a voltage to the motor, which will then attempt to turn at that speed, resulting in a motor load defined by the propellers rotational speed to torque curve at that specific flight speed. It will be assumed, however, for these calculations that the omega – torque curve is known (whether it be for a propeller operating in static conditions or in flight) and thus that omega and torque are the only inputs.

The most important and regular relationship in the motor is the relation between the torque demand and the motor current:

$$I = \frac{Q_{out}}{K_T} + I_{fr} \tag{E.1}$$

Where I is the motor voltage, Q_{out} is the torque output of the motor, K_T is the torque coefficient of the motor and I_{fr} is an additional frictional current, equivalent to the current required to overcome the various sources of friction and losses within the motor. Within the current model the frictional and loss current is modelled using three coefficients, defined through:

$$I_{fr} = k_1\omega^2 + k_2\omega + k_3 \tag{E.2}$$

Here k_1 is a coefficient affecting predominantly turbulent aerodynamic losses in the motor, which become most important at very high speeds. The coefficient k_2 is predominantly determined

from low Reynolds number aerodynamic drag (scaling with velocity rather than velocity squared) resulting from the small Reynolds numbers involved in the bearings. The coefficient k_3 is related to both sliding friction and inductive losses in the motor.

The motor terminal voltage at a certain rotational speed depends mainly on the so called K_v value, also known as back EMF constant, the motor constant, or the speed constant, typically measured in rpm/V (rad/s/V in SI units).

$$V = \frac{\omega}{K_v} + IR \tag{E.3}$$

Where V is motor voltage, ω is the rotational speed in rad/s, K_v is the motor constant in rad/s/V, I is the motor current and R is the motor's internal resistance.

From equations E.1 and E.3 the electrical power consumption of the motor can be calculated through P=VI. It should be noted that the motor K_v and electrical resistance depend on the temperature of the motor magnets and windings respectively, which can change due to a higher initial motor temperature (hot environments) or extended motor operation leading to raised operating temperatures.

For motors where accurate motor characteristics are provided, such as motors produced by AXI, this approach predicts the motor consumption to within 5% of test bench results. Figures E.1 and E.2 show test bench data compared to these equations. The experiments were conducted at the drone company senseFly and the results used with permission. Due to reasons of confidentiality the exact test set up cannot be given here.

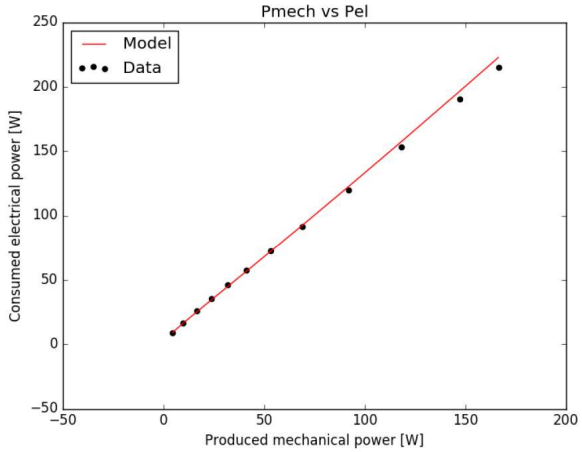

Figure E.1: *Actual test bench consumed electrical power vs resulting electrical power compared to model predictions for an AXI motor.*

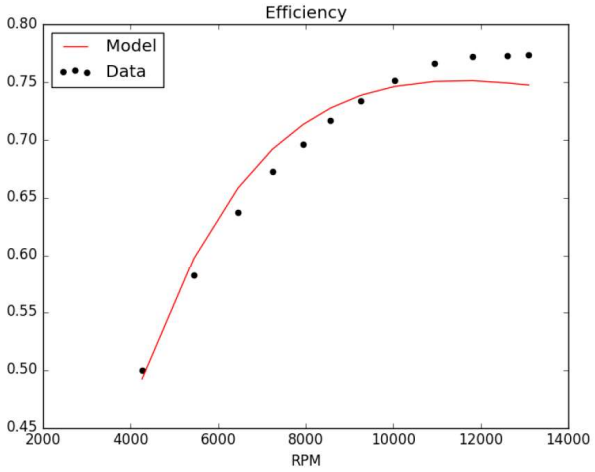

Figure E.2: *Actual test bench mechanical efficiency vs propeller rotations per minute (RPM) compared to model predictions for an AXI motor.*

E.2 Predicting motor and propeller performance and PropPy code

The motor and propeller system is highly interrelated, especially in fixed wing flight, and predicting the system airspeed and electrical power consumption is not a trivial task. A simplified view of the power system from the controller command to the craft airspeed is given in figure E.3 below. The system can be considered as a series of connected components, with the only two inputs being the throttle command and the battery voltage. From these inputs, a corresponding craft airspeed and current draw results. A properly chosen motor and propeller combination will minimise the current draw for a given craft airspeed, which in turn minimises the power consumption and maximises the craft's attainable range. As a typical propeller efficiency can range in the order of 20% to 80% in flight (Brandt and Selig, 2011) and motor efficiency can vary in the order of 0% to 80% (Micromo Micro Motion Solutions, 2010), a poor motor/propeller combination cause power consumption to be several times greater than that of an optimal combination.

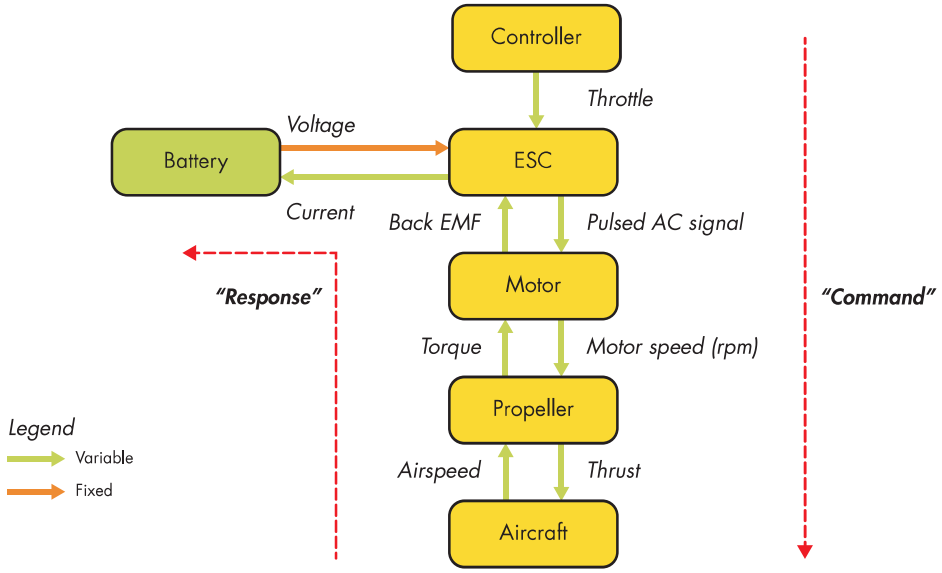

Figure E.3: *Schematic of power system showing relations between components.*

The performance of each component depends on a number of factors. The current pulled from the battery depends on the current used by the motor. The current used by the motor depends on its current speed and torque, as well as its voltage. The torque and thrust of the propeller depends on its current rotational speed and its forward air speed. The airspeed of the plane depends on its drag and the thrust the propeller produces.

Essentially, the battery voltage is fixed by the choice of battery for the craft. The user (or autopilot) will send a throttle command to the Electronic Speed Controller (ESC) which will in turn attempt to drive the motor at a specific speed through a varying AC signal. The motor sends feedback as to its instantaneous position through a varying back EMF voltage, which is used by the ESC in regulating its AC signal. The final speed of the motor will depend on the torque it is attempting to spin at, which is a function of the propeller. The motor torque is the main factor in determining the current it will draw from the battery. The propeller will spin at the same speed as the motor, causing the torque which itself is dependant on the airspeed of the craft. The spinning propeller will result in a thrust, which will result in a steady airspeed where the thrust is equal to the craft's drag at that speed. The entire system is very interconnected and cannot be entirely decoupled.

To predict the power consumption of this highly connected system, a python code has been written to create a model. The performance of the propeller is interpolated and extrapolated from the extensive low Reynolds number propeller data from Brandt and Selig (2011). The motor performance is calculated using the approach detailed in section E above. The drag profile of the aircraft is calculated using the XFLR5 aerodynamic calculation tool. The code written for this project will not be fully detailed in this report more than a brief discussion of the theory. It has been made open source and can be found at `https://github.com/cadowd/proppy`

(approximately 3500 lines of code).

E.2.1 Theory

To calculate the torque and thrust of the propeller spinning at any given RPM and forwards velocity, the wind tunnel test data from the University of Illinois test campaign (Brandt and Selig, 2011) is interpolated and extrapolated. The performance of the propeller can be demonstrated through dimensional analysis to be some function of advance ratio J and Reynolds number Re, defined below:

$$J = \frac{U}{nD}$$

$$Re = \frac{U_{tip} D}{\mu}$$

Where U is the forwards velocity of the air in m/s, U_{tip} is the velocity of the propeller tip (a sum of its forwards and rotational components), n is the rotational frequency in units of 1/s, D is the propeller diameter in meters and μ is the air's dynamic viscosity, slightly dependent on its temperature. The wind tunnel data can be organised to plot the torque and thrust coefficients as a function of these two variables, as in figures E.4 and E.5 below. The torque and thrust coefficients C_Q and C_T respectively are defined as below.

$$C_T = \frac{T}{\rho n^2 D^4} \tag{E.4}$$

$$C_Q = \frac{Q}{\rho n^2 D^5} \tag{E.5}$$

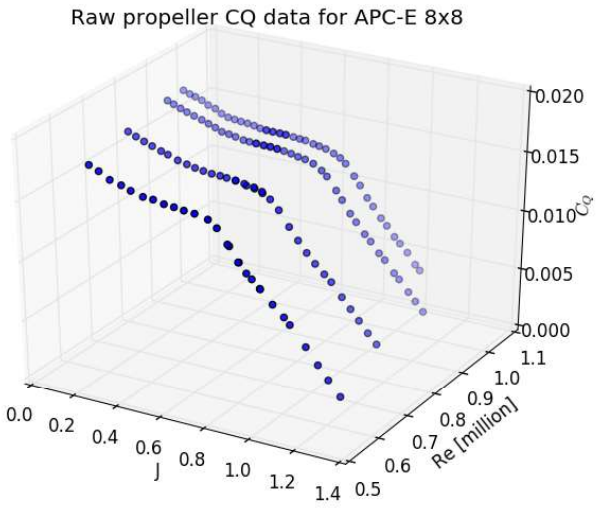

Figure E.4: *Raw windtunnel values of propeller C_Q for an APC 8x8 electric propeller.*

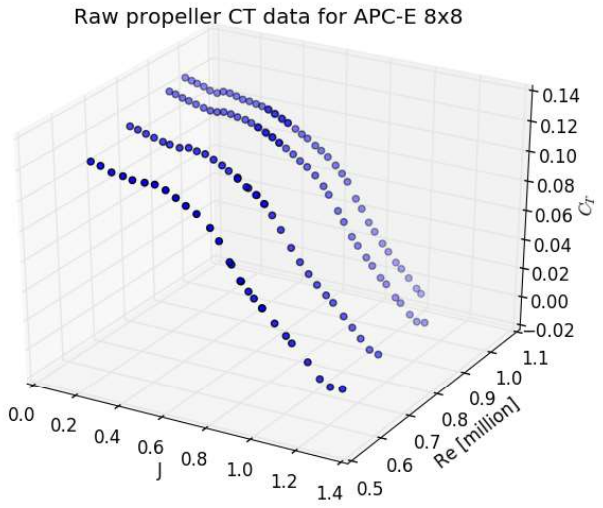

Figure E.5: *Raw windtunnel values of propeller C_T for an APC 8x8 electric propeller.*

These values can be interpolated and extrapolated to give an interpolation surface across all reasonable values of J and Re as shown in figures E.6 and E.7 below.

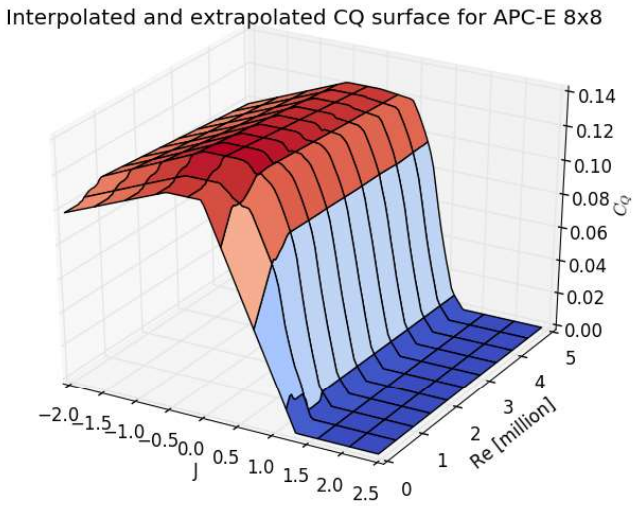

Figure E.6: *Extrapolated and interpolated C_Q surface for an APC 8x8 electric propeller.*

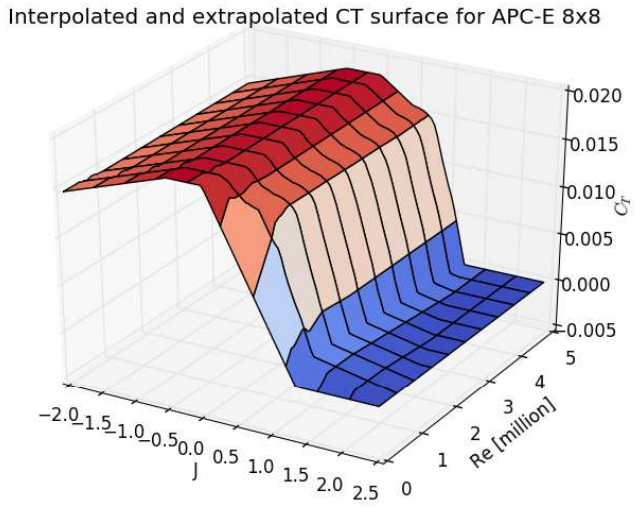

Figure E.7: *Extrapolated and interpolated C_T surface for an APC 8x8 electric propeller.*

As the propeller's diameter is known, these surfaces can be used to calculate a torque and rotational speed for any forwards velocity and thrust value within the considered range of values. These torque and rotational speed values are used as inputs to the BLDC motor equations discussed above in section E to give a current draw for any forwards velocity and thrust. This results in surfaces of electrical power consumption, system efficiency and current for any possible air velocity and system thrust. An example of such an efficiency surface is given in figure E.8 below.

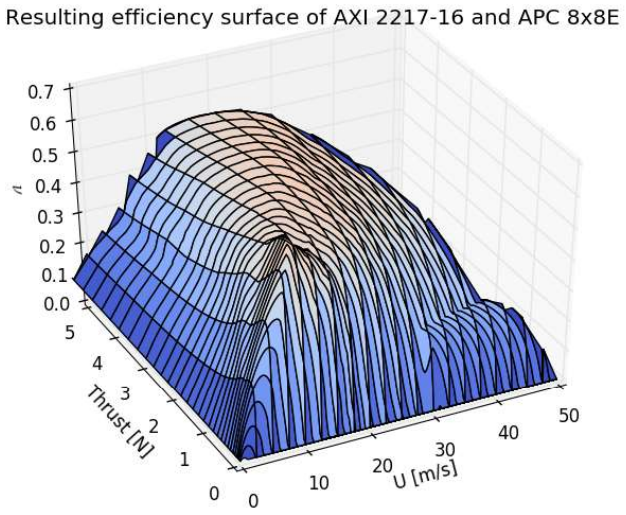

Figure E.8: *Resulting calculated efficiency surface for an APC 8x8 electric propeller and AXI 2817-16 motor.*

Once the drag polar of the aircraft has been calculated by an XFLR5 analysis, the drag of the craft at any given steady airspeed can be calculated. For each of these drag and airspeed points from the drag polar a system consumption, efficiency and current draw can be calculated by interpolating the previously calculated efficiency and power surfaces.

This approach of using interpolation surfaces and finding their intersections allows the calculations to calculate all operating points simultaneously, which significantly speeds up the calculations. This allows multiple viable combinations to be rapidly compared and the optimal motor/propeller combination selected.

E.3 Cruise motor and propeller selection

To select an appropriate motor and propeller for the craft's cruising mode, the drag vs airspeed curve is estimated using the XFLR5 results calculated in section C. This is then fed into the codes described with a large number of motors and propellers compared to find the optimal combination that maximises the vehicle range. The motor data was taken from the manufacturers websites and the propeller data used the University of Illinois wind-tunnel results (Brandt and Selig, 2011). For APC propellers there also exists a large database of simulation results on the APC website. However, these were calculated using a transonic inviscid code which predicts significantly more optimistic values than the wind-tunnel results and so was not used for the propeller selection (Advanced Precision Composites (APC), 2016). The battery voltage was set to 14.8 V, the nominal voltage of a 4S lithium polymer (LiPo) battery.

From the wide selection of motors and propellers initially analysed, it was found that motors with Kv values in the ranges of around 800 to 1400 RPM/V and propellers with high pitches of approximately 8 to 9 inch diameter were optimal. A plot of the regions of maximal efficiency for combinations in this range is shown below in figure E.9. Here efficiency is defined as the distance travelled on a single unit of energy to ensure the range is optimised.

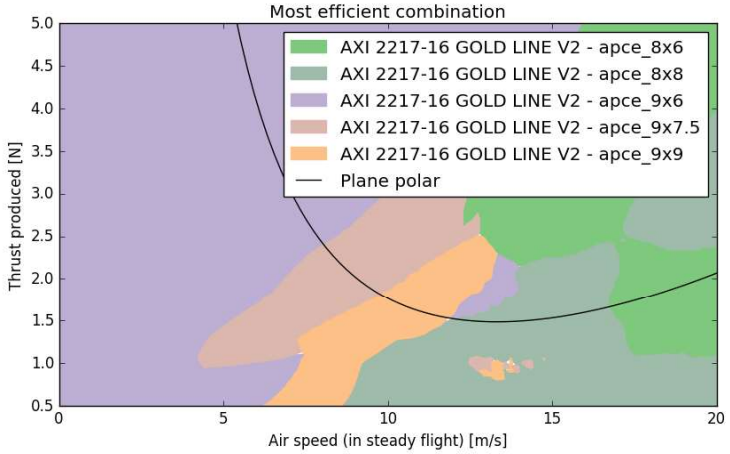

Figure E.9: *Map showing regions of maximum efficiency for selection of available propellers and motors. Plot generated using the PropPy code.*

The AXI motors were found to promise the highest efficiency, with better efficiency at low speeds and high thrusts given by larger, lower pitched propellers and high pitch, small diameter propellers performing better at high speeds and low thrusts. The range of most interest for this craft is the area around the minimum drag, where the AXI 2217-16 motor and APC 8x8 electric series propeller promises better performance. In this same region the APC 9x6 electric series propeller is also promising. This is less visible in figure E.9 as it competes in the same region as the APC 8x8 propeller. The code predicts the 8x8-E propeller to be allow for a 0.3% higher distance travelled per unit of energy, so the difference between these two options is very narrow.

Plotting the efficiency of this combination shows that this combination's region of maximum efficiency corresponds well with the drag 'bucket' of the aircraft and that efficiency is maintained at higher speeds, shown in figure E.10. However, it drops relatively rapidly with increases in thrust(vertical lines on the efficiency contour), especially at lower speeds, so the control of the aircraft should ideally smooth out sudden throttle commands to maintain high efficiency.

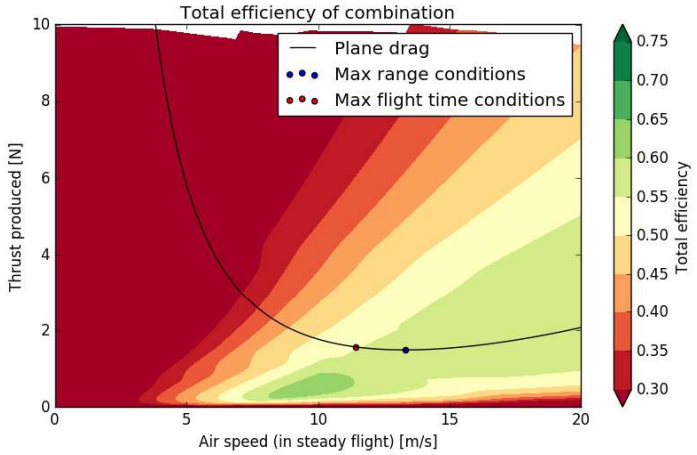

Figure E.10: *Map showing efficiency contours of AXI 2217-16 motor and APC 8x8 electric series propeller. Plot generated using the PropPy code.*

The next most promising combination in this region is the same motor with an APC-E 9x6 propeller. Investigating the efficiency contours for this combination in figure E.11 below reveals that the region of maximum efficiency is approximately the same size, as well as corresponding well to the drag curve of the aircraft. It offers slightly higher efficiency at slower speeds, and approximately 40% more maximum thrust. While the maximum thrust would be of importance for a non-VTOL craft where it plays a major role in take-off characteristics, for a VTOL craft the cruise propulsion is only used to maintain the cruising speed and so the maximum thrust is less critical. The craft will not be required to be highly manoeuvrable in cruise, so the efficiencies at thrusts higher than cruising drag is not of as much interest. The code does predict a longer maximal flight time with this combination (as the most efficiency cruise speed is slightly lower).

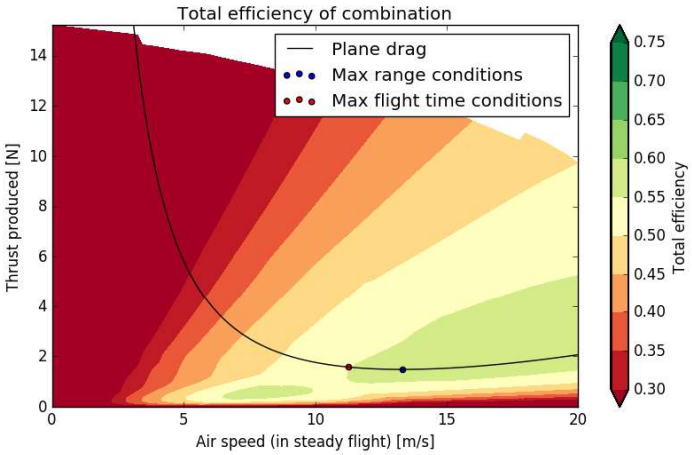

Figure E.11: *Map showing efficiency contours of AXI 2217-16 motor and APC 9x6 electric series propeller. Plot generated using the PropPy code.*

Despite the higher available thrust possible with the 9x6 propeller and better efficiency at low speeds, the 8x8 propeller will be chosen due to its marginally better performance at cruising speed. This will need to be verified by flight testing and ideally both propellers would be investigated for consumption should time allow.

Unfortunately, the propeller databases did not include data on folding propellers, which will ultimately be the propeller implemented in order to ensure compact folding. However, the company Aeronaut produces a folding propeller of equivalent diameter and pitch which will be assumed to offer approximately equivalent performance. The part itself consists of 8 inch blade with 7 inch pitch by default, although the propeller yoke has the option of an additional 2.5° rotation which results in an equivalent 8x8 propeller according to the Aeronaut datasheets (Aero-naut, 2016).

The power consumed by the two considered combinations is shown below in figure E.12. At cruising speeds the power consumption is estimated to be approximately 33 W for both combinations. The 9x6 propeller draws lower power at lower speeds compared to the 8x8, although the 8x8 is more efficient at higher speeds (due to its higher pitch) and results in a higher top speed.

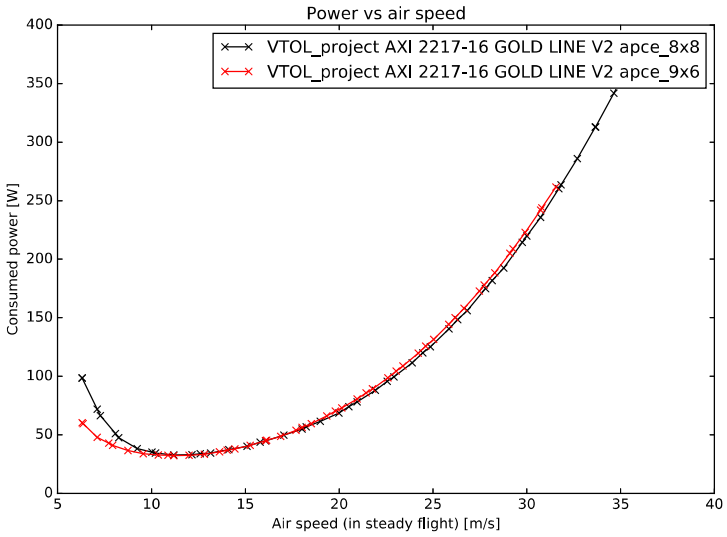

Figure E.12: *Plot of electric power consumption vs steady flight speed. Plot generated using the PropPy code.*

The plot of figure E.12 also shows the predicted range of flight speeds for the craft. The lower speeds are at a high angle of attack where stall is likely, so a significant margin of error must be added to avoid operating in this regime (the exact onset of stall is poorly predicted in panel methods such as those used in XFLR5). At higher speeds the higher order effects not accounted for in the model as well as additional drag sources (such as the fuselage and other unmodelled protrusions) begin to contribute more to the total drag, so the craft is unlikely to actually be able to reach these extremes. A conservative estimate of the minimum speed is 10m/s, which will be used as the transition speed from hovering to cruise flight.

E.3.1 Effect of mass on flight

Currently the main limit to the take-off mass of the craft is the hovering thrust. If this restriction is ignored, the airframe is able to support much larger payloads, being limited only by its cruising power and its structural strength.

Figure E.13 shows a comparison of the power consumption in steady flight for the airframe at different total masses, using its drag polar extracted from the XFLR5 analysis and the motor and propeller selected above. It is evident that increasing the mass increases the power consumption, as well as increasing the necessary transition speed. Note that in this analysis the hovering power consumption is neglected. Also note that the AXI 2217/16 motor is limited to 245W power without the risk of overheating.

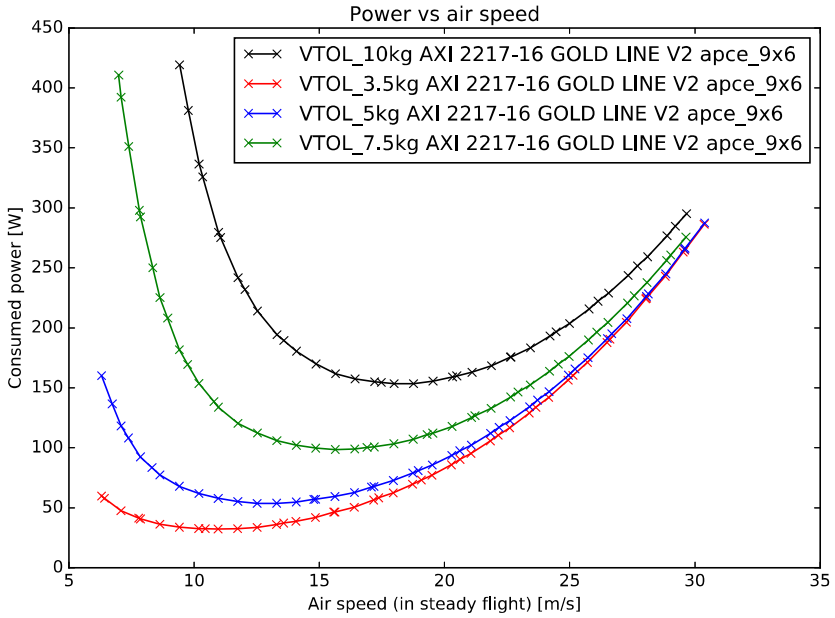

Figure E.13: *Effects of increased airframe mass on power consumption.*

Using these results, the total range of the craft for each mass can be calculated. The take-off power is neglected (as this will change in a non-linear fashion with mass); however, the 6.25 amp hour battery selected in section F is used for the distance calculation. The results are shown in table E.1.

Table E.1: *Effect of vehicle mass on cruise range*

Airframe mass [kg]	3.5	5	7.5	10
Cruise speed [m/s]	13.2	13.02	15.66	18.5
Cruise power [W]	40	56	100	155
Total range [km]	109.89	77.42	52.14	39.74

It is clear that the mass of the craft can reasonably increased up to 5kg without a significant impact on its cruising efficiency and total range, although above 7.5kg the range reduces significantly. To increase the payload of the design more powerful rotors are therefore required. It should be noted that this analysis does not account for the necessary increases in structural strength to support the additional mass, tests would have to be performed to confirm that the airframe can support an increase in mass.

E.4 Hover motor and propulsion selection

The hover motors need to generate a maximum thrust of approximately 1.75 kg, and be most efficient while generating a thrust of 1.4kg (see appendix D). Again using the PropPy code developed (see appendix E.2), the power consumption of different propeller and motor com-

binations at different thrusts can be plotted. As wind-tunnel data is not available from the UI propeller database for large multi-rotor propellers, the simulated wind-tunnel data from the APC website was used for these calculations (Advanced Precision Composites (APC), 2016). Comparisons within the program have shown power consumptions calculated using this data to be approximately 20% lower than results using the UI data.

It should be noted that it is not important to select the hover motor system for a top speed, as the thrust for forwards flight is also generated by the cruise motor which will be easily sufficient to allow the vehicle to reach its transition speed.

To begin the motor selection, an idea of the Kv value is required. It is already known that the propeller blade will be 12 inches in diameter. Typical C_T and C_P values for propellers in this size are approximately 0.08 and 0.04 respectively (Deters and Selig, 2008). Using equations C.1 and C.2 given in section C, the propeller can therefore be expected to spin at around 8700 RPM and require about 388W of mechanical power. Assuming the motor to be about 70% efficient, this should be about 550W of electrical power.

Using the equation for voltage and Kv given in the brushless motor section E (equation E.3) and assuming an ideal motor with no electrical resistance (for the moment), the minimum Kv value for the motor is therefore 590 RPM/V. This is the minimum Kv value for a motor to achieve sufficient thrust with the approximate 12 inch propeller described. Real motors will need a Kv higher than this, with their efficiency increasing with lower values of internal resistance. An appropriate real motor will also need to be rated to approximately 550W of power.

A range of available motors from Hobbyking and other online stores were selected according to this criteria to form a short list of motors for comparison. These motors had Kv values between 590 and 800, and were all rated to 550W. The PropPy code was used to compare these motors with a range of 12 inch propellers, with the top performing combinations plotted in figure E.14.

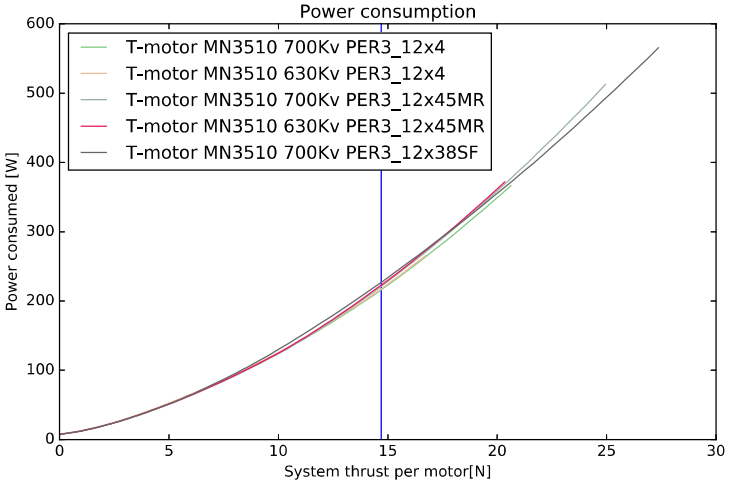

Figure E.14: *Plot of electric power consumption vs steady flight speed. Plot generated using the PropPy code.*

The most efficient combination at the specified thrust (1.5kg in hover, see section D) is the T-motor MN3510 using an APC 12x4 propeller. It has a maximum thrust of 21.5 N according to this model. Bench tests are required to verify these results. For the prototype, however, this is the combination which has been selected. As the APC 12x4 propellers are not available in both pusher and tractor orientations, the T-motor carbon 12x4 propeller is used instead and is assumed to perform similarly to the calculations.

For the rear motor, the thrust required is only 875g at full throttle (see appendix D) and so a 640 Kv motor is used (as it will pull less current at the same torque and therefore less current for a similar thrust compared to the 700 Kv motor). This limits the maximum thrust possible of the rear motor to approximately 17N (1.7kg) according to figure E.14, however, this is more than enough according to the balance calculations.